Annual Review of Fluid Mechanics

Ocean Wave Interactions with Sea Ice: A Reappraisal

Vernon A. Squire

Department of Mathematics and Statistics, University of Otago, Dunedin 9016, New Zealand; email: vernon.squire@otago.ac.nz

Annu. Rev. Fluid Mech. 2020. 52:37–60

First published as a Review in Advance on June 21, 2019

The *Annual Review of Fluid Mechanics* is online at fluid.annualreviews.org

https://doi.org/10.1146/annurev-fluid-010719-060301

Keywords

surface gravity waves, sea ice, polar and subpolar seas, climate change

Abstract

A spectacular resurgence of interest in the topic of ocean wave/sea ice interactions has unfolded over the last two decades, fueled primarily by the deleterious ramifications of global climate change on the polar seas. The Arctic is particularly affected, with a widespread reduction of the extent, thickness, and compactness of its sea ice during the summer, creating an ice cover that is analogous to that in the Southern Ocean surrounding Antarctica. With the additional fetches over which waves can form and mature within more open ice fields, there has also been a documented global uptrend of winds and wave height, which is most severe at high latitudes. Bigger ocean waves affect the way sea ice forms, contribute to how the ice edge moves, penetrate farther into the sea ice, have more destructive power to break up the ice and to change the distribution of floe sizes because the ice is weaker, and assist in lateral melting. These feedbacks collectively identify a parametrization currently absent from Earth system models, as well as shortcomings in wave forecasts arising from limited understanding of the impact of sea ice on ocean waves.

1. INTRODUCTION

1.1. Context

Landfast ice: sea ice fastened to the coastline, the sea floor along shoals, or grounded icebergs

Ice floe: a separate patch of floating sea ice or flat sheet of unbroken pack ice, greater than 20 m across

MIZ: marginal ice zone, defined as the region of the ice cover that is substantially affected by open ocean processes

ESMs: Earth system models simulate the atmosphere, oceans, and seas, including their biogeochemistry, the land surface with its vegetation, sea ice, and terrestrial ice

Pack ice: ice that is not attached to the shoreline and drifts in response to winds, currents, and other forces

Pancake ice: cakes of approximately circular new ice, up to 100 mm thick and 0.03–3 m in diameter, with raised edges; formed from the freezing together of grease ice

Nilas: a thin sheet of smooth, flexible level ice less than 100 mm thick, which appears dark when thin

Frazil: fine spicules or plates of ice in suspension in water

The transmission of ocean waves into and within different types of sea ice is a well-established geophysical research topic, which is currently attracting renewed attention as a result of recent adjustments to the Earth's marine ice covers that are occurring because of global climate warming. Two reviews have already been published that synthesize historical progress in the field of ocean wave/sea ice interactions, namely, that of Squire et al. (1995) and the mostly theoretical corpus of research described by Squire (2007). These reviews include exhaustive bibliographies that catalog early progress in the field, with commentaries from the heroic era of exploration, experimental studies in the 1930s, the introduction of mathematical sophistication in the 1950s and late 1960s, the influential work of Wadhams and others in the 1970s and 1980s—especially studies done under the aegis of the MIZEX (Marginal Ice Zone Experiment) campaign—and more recent developments utilizing powerful theoretical and numerical solution methods for both landfast sea ice and the modestly sized ice floes of the marginal ice zone (MIZ). In this review, I avoid discussing material covered by Squire et al. (1995) and Squire (2007) unless it is necessary to shed light on specific aspects of more recent publications. There are ancillary narratives that touch on this topic, including encyclopedic précis (e.g., Shen 2017) and Weeks's (2010) meticulously comprehensive book on sea ice. Russian work is also plentiful, helpfully summarized in the excellent book by Bukatov (2017), which is available open access in Russian from the Marine Hydrophysical Institute of the Russian Academy of Sciences.

While climate change has affected the sea ice of both hemispheres, it has been especially pronounced in the Arctic, where the composition of summer sea ice, in particular, has evolved to be less compact and may in fact be becoming more like Antarctic sea ice. In this context, humankind's knowledge about how ocean waves interact with sea ice in its various forms has been majorly influenced by a timely initiative of the US Office of Naval Research. Entitled "Sea State and Boundary Layer Physics of the Emerging Arctic Ocean" [henceforth "Arctic Sea State"; see Thomson et al. (2013) for the science plan] and including a complementary field campaign in the Beaufort Sea during 2015, this program's goals were to (*a*) understand the changing surface wave and wind climate in the western Arctic, (*b*) improve numerical and theoretical models of wave–ice interactions, (*c*) quantify the fluxes of heat and momentum at the air–ice–ocean interface, and (*d*) apply the results in coupled forecast models (Thomson et al. 2018).

Because higher waves are now occurring more often as a result of the increased frequency and intensity of storms, the ingress of ocean waves into sea ice fields is potentially more destructive than before. Waves can also grow throughout the ice cover itself due to the presence of more open water and hence increased fetches over which waves can form and mature. To be credible, Earth system models (ESMs), ice/ocean models, and wave forecasting parameterizations should assimilate this physics, which they currently do either superficially or not at all. Recognizing that (*a*) ice–albedo feedback (see, e.g., Deser et al. 2000) will be assisted by ocean waves, which alter atmosphere/ice/ocean fluxes by breaking up ice, and (*b*) wave stress is of similar order to wind stress over large areas of the MIZ, making wave forcing significant for the MIZ's overall dynamics (see **Figure 1**), the omission of wave–ice interactions is likely to be a contributor to the disagreement between climate model simulations and observations reported by Stroeve et al. (2007).

Whether focused upon continuous pack ice, the loosely compacted ice floes of the MIZ, or pancake ice, nilas, frazil, and grease ice, the compilation of research papers and reports is impressive and continues to grow as the contemporary importance of the subject is recognized and technological advances make practicable more sophisticated measurements that were not feasible 20 years ago.

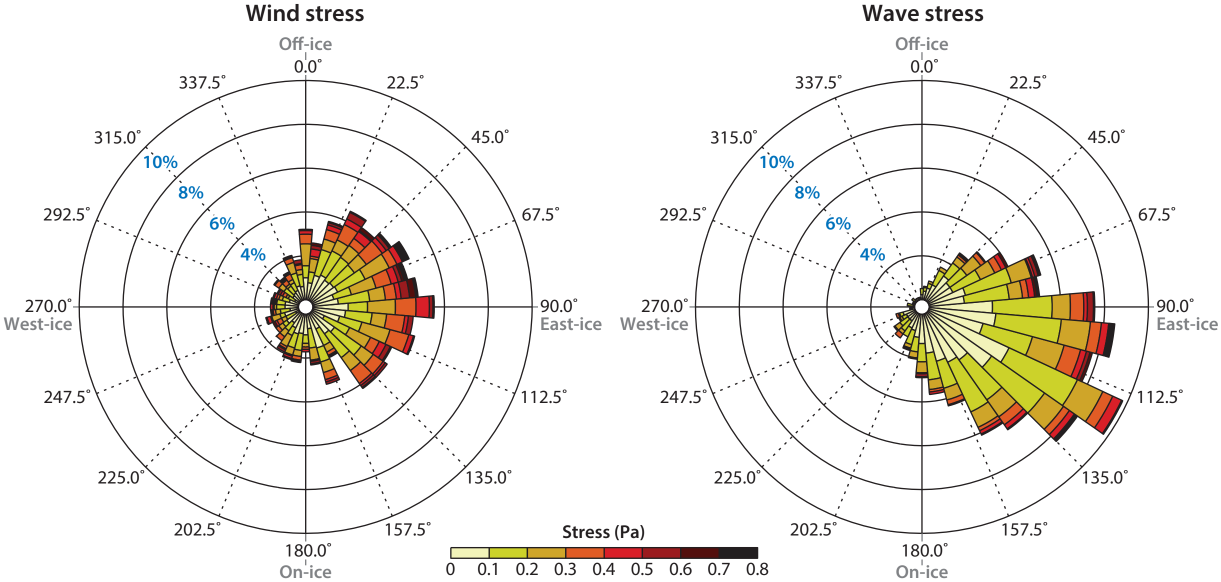

Figure 1

Wind stress computed from the Climate Forecast System Reanalysis (*left*) and wave stress at 10 km inside the ice edge computed from Sentinel-1 synthetic aperture radars (*right*), as functions of probability, magnitude, and direction relative to the ice edge. Wind and wave stress vectors both flow toward the directions indicated. Figure adapted with permission from Stopa et al. (2018b).

1.2. How Sea Ice Affects Waves

When ocean waves travel in an ice cover, whether composed of the discrete ice floes that exemplify the MIZ or forming a continuous sheet, they decrease in amplitude at a rate determined by the nature of the sea ice. The reduction arises due to a combination of two processes, scattering and dissipation, both of which need to be accommodated in any ESM, ice/ocean model, or wave forecasting parameterization. Scattering redistributes energy but does not eliminate it, while dissipation, insofar as the waves are concerned, removes energy. (The latter process actually reassigns the energy to other parts of the atmosphere/ice/water system, e.g., to kinetic energy in the mixed layer, etc., which is important for ESMs that are required to conserve energy because they compute results over very long timescales. However, this subtlety is not important here, as the system under consideration is not closed.) Dissipation is due to an abundance of processes that are symptomatic of a MIZ. We expect considerable turbulence; inelastic ice floe collisions that can include reducing the ice to a slurry by pummeling; vortex shedding; wave breaking, overtopping, and repetitive overwashing of the floes; spontaneous green water at large wave amplitudes; energy loss associated with ice deformation under extreme conditions; ridging, rafting, and ice floe fracture; and other less obvious mechanisms. Near the ice edge, when the seas are rough, considerable destruction of the ice floes can occur, but because the dissipation eliminates higher frequency waves before lower frequency ones, the zone of intense energy loss is typically limited to approximately 10–20 km in Arctic waters (Squire & Moore 1980). In Antarctica's Southern Ocean, where seas are much fiercer, the zone of destruction is considerably broader. The attenuation rates in these outer zones likely deviate significantly from those in the interior and may even have a different functional dependence on the distance traveled by the waves. It is also conjectured that large-amplitude waves may appear to attenuate differently from those with smaller amplitudes (Li et al. 2015a, Squire 2018),

Grease ice: a soupy layer of frazil crystals clumped together, which makes the ocean surface resemble an oil slick

Green water: a large quantity of turbulent water on a floating body's surface as a result of massive waves during a large storm as the effects of wind input, nonlinear interaction, and nonlinear dissipation mechanisms such as overwash and wave breaking will be more pronounced.

WW3: WAVEWATCH III® wave forecasting system

The energy transport equation, or the wave action equation in WAVEWATCH III® (WW3) where ocean currents are included (WW3DG 2016), is used to embed ocean waves in large-scale models. We express this equation in its simplest notional form for energy density $E = E(\mathbf{x}, \omega, \theta)$,

$$(\partial_t + \mathbf{c}_\mathrm{g}.\nabla)E = \sum S = S_\mathrm{in} + S_\mathrm{nl} + S_\mathrm{ds} + S_\mathrm{ice}, \qquad 1.$$

where $\mathbf{x}$ denotes the spatial coordinates, ω is the radian frequency (equal to $2\pi f = 2\pi/T$, where f is the frequency in hertz and T is the wave period in seconds), θ is the direction of travel of the wave, the group velocity vector $\mathbf{c}_\mathrm{g}$ is a function of ω but here is taken as a constant in space and time, and $\sum S$ encapsulates several source/sink terms defined as functions of ω, described as follows. The term S_in represents wind–wave interaction, S_nl is a nonlinear wave–wave interaction term, S_ds is a dissipation (whitecapping) term, and $S_\mathrm{ice} = S_\mathrm{ice}(\mathbf{x}, \omega, \theta)$ is the term of interest in this work, as it characterizes how the waves are affected by the ice field. The term S_ice can be partitioned into the two processes introduced above, respectively designated energy attenuation coefficients α_scat and α_dis,

$$S_\mathrm{ice} = -c_\mathrm{g}E\,(\alpha_\mathrm{scat} + \alpha_\mathrm{dis}) + c_\mathrm{g}\int_0^{2\pi} EK(\theta - \theta')\,\mathrm{d}\theta', \qquad 2.$$

such that $\int_0^{2\pi} S_\mathrm{ice}\,\mathrm{d}\theta$ and $-\alpha_\mathrm{scat} + \int_0^{2\pi} K(\theta - \theta')\,\mathrm{d}\theta'$ both equal zero for $\alpha_\mathrm{dis} = 0$, where K is the scattering kernel.

I have specifically referred to α_scat and α_dis as energy attenuation coefficients, in keeping with WW3DG (2016). Since many theoretical papers are developed in terms of amplitude, to avoid ambiguity, I mention in passing that the amplitude attenuation coefficient k_i of the primary propagating monochromatic wave is often quoted (see below). For the exponential attenuation that is commonly observed when ocean waves pass through sea ice fields, the energy attenuation coefficient is twice the amplitude attenuation coefficient because energy density is proportional to the square of the wave amplitude.

Most theoretical models constructed to describe how sea ice affects waves or vice versa are configured to fit a linear paradigm. They employ an Airy wave mode ansatz of the form $A \exp \mathrm{i}(kx \pm \omega t)$, where A is the initial wave amplitude, x is the direction of propagation, and t is time. The generic wave number, $k = \kappa + \mathrm{i}\,k_\mathrm{i}$, defines propagation either in the water or beneath the ice cover and encapsulates dispersion (via the real quantity κ) and attenuation due to the presence of the sea ice (via imaginary $\mathrm{i}\,k_\mathrm{i}$) into one consolidated complex wave number. Because sea ice is compliant, the ice plate itself deforms as the ocean wave passes beneath. As a rule, the sea ice is presumed to be elastic, viscous, or viscoelastic; each assumption is reasonable when the wave amplitudes are modest for the strain rates induced by typical surface waves in the sea ice under various circumstances. The material properties chosen for the sea ice provide the dispersion relation that regulates (*a*) how the waves propagate under the ice cover (i.e., how they disperse and reduce in amplitude) and (*b*) the reflection coefficients at interfaces between open water and ice or changes in ice morphology, as the wave numbers in each medium are different (Fox & Squire 1994). Weakly nonlinear formulations exist but are relatively rare (Hegarty & Squire 2008).

Considerable modeling work has been done over several years to understand α_scat, most recently for the MIZ; this work is built on an appreciable body of hydroelastic research that dates back decades and focuses for the most part on scattering from imperfections in continuous sea ice or from ensembles of floating bodies with typically uncomplicated shapes and configurations (see Squire 2007). For solid ice floes or ice sheets, the deformation is substantially elastic at the strain rates induced by the waves, so hydroelastic theory is applicable. However, even with the pervasive simplifying assumption that ice sheets and ice floes behave as classical Kirchhoff–Love plates, the mathematics is not trivial because the set of admissible wave modes differs across each interface. A primary propagating wave mode plus an infinite set of evanescent wave modes exist in water with a free surface, but for ice-covered sea and depending on the physical and material properties of the ice, there is a primary propagating wave mode, a complex conjugate pair of decaying propagating modes, and an infinite set of evanescent modes. Modes must be matched across every interface. Most scattering occurs when ice length scales and ocean wavelengths are of similar order.

Although it is recognized that such scattering models are never perfect, I feel that the redistribution of wave energy that occurs due to scattering by floes in MIZs, which results in attenuation of the primary propagating wave field expressed through the coefficient α_{scat} and associated changes to directional spread, is well understood and adequately modeled. This is important because contemporary phase-resolving scattering models provide a direct link to ice floe breakup and hence to how the floe size distribution (FSD) changes, via the flexural stresses in the compliant ice floes that make up the MIZ. The link back to the scattering kernel $K(\theta - \theta')$ in Equation 2 is an imperative of phase-resolving models that is of particular importance to WW3.

Kirchhoff–Love elastic plate: an extension of Euler–Bernoulli beam theory to plates; the theory assumes that a mid-surface plane can be used to represent a 3D plate in 2D form

FSD: floe size distribution, usually expressed as a probability density function of floe sizes

Unconsolidated suspensions such as pancake ice and frazil slurries have characteristic length scales that are much smaller than ocean wavelengths, and they are normally less resilient than solid ice, with a major viscous component that causes $\alpha_{\text{dis}} \gg \alpha_{\text{scat}}$. As a result, waves passing through these types of ice are not scattered to any extent. Regrettably, there are presently no comparable satisfactory, physically defensible models to quantify α_{dis}, and creating a viable model to fit the multifarious realizations of the MIZ is unlikely to be achievable, as the contribution from the numerous dissipative mechanisms changes with both the wave and the ice conditions. Moreover, despite our tolerable mastery of the scattered fields, potentially very energetic dissipation will also occur in the waters between floes as a result of the scattering process itself. The convenience of separating α_{scat} and α_{dis} in Equation 2 may then become unpalatable, although we accept its utility.

Yet, apparently the sea ice and the waves are uninformed of my skepticism, as a simple low-order power law with a power index dependent on ice conditions appears consistently to describe how attenuation varies with wave frequency in field observations, as illustrated in **Figure 2** (Meylan et al. 2018). Unfortunately, to my knowledge, no dissipative model has convincingly reproduced this proportionality to date; indeed, most are asymptotically way off the mark, and it may be that a homogeneous linear model will never accurately reproduce what is observed.

As far as possible, I have separated the remaining sections of this review into a logical framework that allows readers to target their specific area of interest. Section 2 discusses the two prominent classes of theoretical models in the field: more or less what Squire (2018) identifies as paradigm I models, which attempt to replicate the physics, and paradigm II models, which parameterize phenomena for expediency (although the link to Squire's terminology is incidental). Nonlinear analyses, although uncommon, are included. Experiments conducted in the field in situ, remotely using satellite or aircraft, and in the laboratory are reported in Section 3. There is an overlap between Sections 2 and 3 because theory is often developed alongside an experiment to interpret and explain the data set collected. I have also included a short Section 4 on early attempts to embed features of wave–ice interactions in large-scale models, e.g., ESMs and wave forecasting models such as WW3.

2. THEORETICAL MODELS OF WAVE–ICE INTERACTION

As mentioned in Section 1.1, many of the advances reported here proceed from a sequence of earlier works that developed mathematical techniques to determine how sea waves reflect from ice

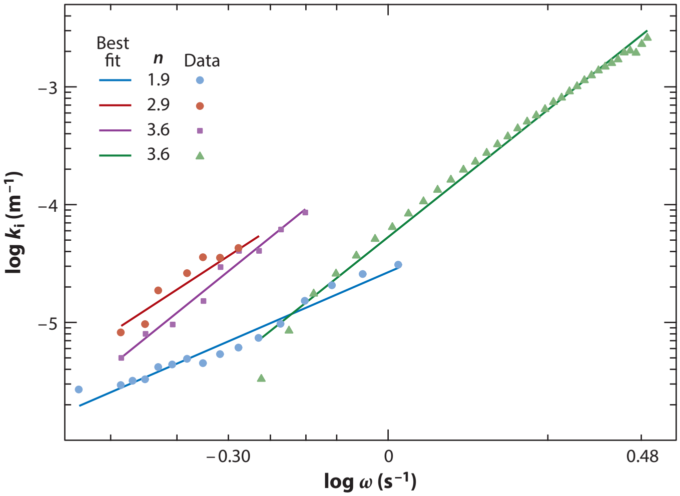

Figure 2

Log–log plots of median values of the amplitude attenuation coefficient k_{i} versus radian frequency $\omega = 2\pi f$ (*markers*), overlaid with best fits of the form $k_{\mathrm{i}} \propto \omega^n$ from four independent field experiments. Figure adapted with permission from Meylan et al. (2018).

sheet edges; from imperfections in continuous ice such as cracks, leads, pressure ridges, changes of thickness or property, etc.; from many such scatterers; or from multiple ice floes that, for computational reasons, are simply shaped, identical, or exist in a well-defined structural pattern. Squire (2007) includes an extensive bibliography that lists these publications. Prompted by climate change–induced effects, there has recently been a trend away from continuous sheets of sea ice toward modeling aggregations of ice floes in MIZs. A small number of recent papers have influenced this trend by introducing or finessing new mathematical tools or numerical procedures (e.g., Bennetts et al. 2007).

Leads: long, sinuous open water openings in the sea ice cover, from a few meters to tens of kilometers across, that are formed when ice sheets are pulled apart

Pressure ridge: a hillock above the level surface of the sea ice caused by winds and currents compressing or shearing the ice; an associated keel forms below the ice

2.1. Ice Floes: Single and Multiple

My primary focus here is on modeling how ocean waves interact with single ice floes or with the vast numbers of those floes that are present in the MIZ. However, landfast sea ice is also present along coastlines and particularly in embayments such as harbors, where waves can enter and flex the ice to become what are commonly called ice-coupled waves or flexural gravity waves, potentially causing it to break up.

2.1.1. Continuous sea ice. Notwithstanding its progression to be more like a MIZ during the summer months as a result of global warming, the sea ice of the Arctic Basin is quasi-continuous over large stretches of the ocean. Landfast ice is another example of this type of sea ice, commonly present over a shelving sea floor. Bennetts et al. (2007) used a Rayleigh–Ritz analysis to model these situations, recognizing the limitations of assuming that the floating ice sheet behaves as a homogeneous thin elastic plate, but allowing a finite number of the infinite set of eigenfunctions that support evanescent waves to be included in the expansion and considering both total and partial ice sheet geometries with draft. Although this multimode theory is three-dimensional (3D), Bennetts et al. (2007) demonstrated its use for a 2D bed shape and ice shape subjected to obliquely incident waves.

Bennetts et al. (2009) modeled a periodic structure of finite width embedded within an otherwise uniform 2D system consisting of finite-depth fluid covered by a thin elastic plate. The work is similar in concept to that of Bennetts et al. (2007) but uses transfer matrices to provide a single-mode approximation in which the vertical mode chosen is the one that supports the incident wave. The method employed is accurate and computationally efficient when tested against the multimode theory, but periodic ice terrain is unphysical.

Although both Bennetts et al. papers included the Archimedean draft, i.e., the sea ice was in hydrostatic equilibrium, it was neglected in the vast majority of earlier papers on the basis that ocean wavelengths are very long compared to ice thickness. This assumption has been tested and shown to be true for most sea ice by Williams & Squire (2008) using an entirely different mathematical theory based upon Green's functions that has the advantage of automatically assimilating all modes to full precision. However, significant changes of localized thickness due to a trapped iceberg or massive pressure ridge, for example, or the cumulative effect of many irregularities such as open or refrozen leads and pressure ridges in sea ice (see, e.g., Bennetts & Squire 2012a,b), will undoubtedly cause differences between the zero and nonzero draft theories. The latter effect was investigated by Squire & Williams (2008). In fact, the more complete theory gave Williams & Squire (2010) confidence to test whether ocean waves traveling beneath a sea ice sheet can be used as a technique to remotely sense the ice thickness, on the basis that theory had reached a point where the inherent heterogeneity—expressed as pressure ridge keels and sails, leads, thickness variations, and changes of material property and draft—can be fully assimilated exactly or through approximations whose limitations are understood. It was found that the underlying thickness can be determined to good accuracy by the method as long as the draft is correctly provided for, suggesting that waves can indeed be effective as a remote sensing agent to measure ice thickness in areas where pressure ridges are modest, i.e., away from coastal regions of high deformation.

Polynya: irregularly shaped areas of persistent open water that are sustained by winds or ocean heat, which often occur near coasts, landfast ice, or ice shelves

Using Green's functions methodology, Vaughan & Squire (2007) synthesized the mathematics and numerical techniques just discussed and applied them to 1D scattering of ice-coupled waves by a region of arbitrarily varying thickness. An ensemble of ice sheets was constructed for combinations of the physical parameters that describe the ice sheet, which was then used to show that the reflection coefficient is best described by the ensemble median of the distribution. Of significance, the authors went on to introduce upward-pointing sonar data collected during submarine cruises under Arctic sea ice (NSIDC 2006). This is a theme that was developed by Vaughan & Squire (2008), again with a Green's function solution; by Vaughan et al. (2009), invoking the more sophisticated theory of Bennetts et al. (2007) with viscosity included for generality; and by Squire et al. (2009), who actually modeled waves transiting 1,670 km of real Arctic Ocean sea ice at typical ocean wave periods and computed the attenuation coefficient per meter, $k_i(T) = 0.02\,e^{-0.386T}$, as opposed to the power law relationship, demonstrated in **Figure 2**, that is observed in MIZs.

2.1.2. Single ice floes. While research into the seakeeping performance and flexure of single floes has dwindled, the ensuant mathematical solutions form the kernel of phase-preserving analyses to compute scattering and hence the attenuation coefficient $k_i = k_i(\omega)$ or $\alpha_{scat} = \alpha_{scat}(\omega)$ across entire MIZs, recalling that $\omega = 2\pi f = 2\pi/T$. For example, Montiel et al. (2013a,b) validated a useful linear numerical model of wave interactions with floating compliant discs in a series of wave basin experiments. The most sophisticated model to date (Bennetts & Williams 2010) actually permits the boundary between the ice-covered and free surface fluid regions to be described by an arbitrary smooth curve. This allows the deflection and the diffracted wave field to be found for quite oddly shaped ice floes, and an equivalent calculation can be done for a polynya within an otherwise continuous ice sheet. Although the method is efficient, extrapolation to the tens of thousands of ice floes that constitute a MIZ is impracticable.

Finally, I mention the small amount of nonlinear work that has been done on solitary ice floes; for example, Skene et al. (2015) have successfully used the nonlinear shallow water equations to model the periodic overwashing of the surface of an artificial floe. Especially at the outer regions of the MIZ where incident ocean waves have generally not yet been attenuated to any degree, the modest freeboard of the majority of ice floes makes overwash an important agent to consider.

2.1.3. Multiple ice floes.

Recall comments made in Section 1.2 about our good theoretical understanding of α_{scat} but the dearth of physical models available to quantify α_{dis}. Recall also that scattering doesn't remove energy from ocean waves that pass through the mélange of ice floes that comprise a MIZ; instead the energy is redistributed by reflections on entry to the ice field and then multiple reflections within the MIZ.

Scattering models constructed to determine α_{scat}, which seek to explain field observations of attenuation that date back to the 1970s, are reasonably abundant [reported by Squire et al. (1995) and Squire (2007) prior to around 2007]. The primary challenge has always been the very large number of ice floes available to scatter the wave energy. Either the reflecting elements of the ice field are presumed to be parallel, i.e., one horizontal and one vertical dimension are assumed (Kohout et al. 2007, 2011; Kohout & Meylan 2008; Bennetts & Squire 2012a,b), or the ice in the MIZ is assumed to have a structure that allows a solution to be found to good accuracy in a reasonable time, e.g., periodicity (see, e.g., Peter & Meylan 2007, Wang et al. 2007, Bennetts & Squire 2009, Bennetts et al. 2010). Infinite and semi-infinite MIZs populated by different floe shapes have been modeled in the latter cases, allowing insights into what might occur in real MIZs and prompting a satisfying trend toward ever more mathematical and computational sophistication. A crucial ingredient of these works is the seminal paper by Kagemoto & Yue (1986), which develops an interaction theory assuming linearized potential flow for 3D water wave diffraction and radiation from several nonoverlapping elements.

The most recent works address the issue of the huge number of scatterers in the prototypical MIZ, first for the simpler Helmholtz problem (Montiel et al. 2015a) but later for the MIZ itself (Montiel et al. 2015b, 2016). This is done by partitioning the ice field into a series of contiguous strips of floes parallel to the ice edge that stretch into the interior (**Figure 3*a–c***). By this means, one can construct a phase-resolving linear theory to compute scattering from arrays of $\mathcal{O}(10^3–10^5)$ randomized circular floes, speculating that any impact of the circular geometry will be neutralized by the vast number of scattering events that occurs. To build this model, one first matches the pressure and velocity fields at the interface between the ice-covered and ice-free domains for a single floe, using a local coordinate system. Next, Kagemoto & Yue (1986) interaction theory is invoked for cylindrical waves to express the wave forcing on each ice floe as the coherent sum of the ambient incident wave and the scattered wave fields originating from all the other ice floes in each strip (**Figure 3*d***). The resulting solution is expressed in terms of cylindrical wave forms radiating from all floes in the strip. Finally, the strips are combined by solving a multiple 1D reflection/transmission problem, as each strip partially reflects and transmits the evolving directional wave spectrum radiating from preceding adjacent strips. With good information about the sea ice and the incoming directional wave field, the Montiel et al. (2016) model calculates the attenuation coefficient $\alpha_{\text{scat}}(f)$, adjustments to directionality as the waves enter and transit the MIZ, and the consequent gradual transformation of the FSD (Montiel & Squire 2017). While improved models to compute $\alpha_{\text{scat}}(f)$ will no doubt be developed, for example by removing the circularity assumption, comparisons between current theory and data when scattering dominates, e.g., those done during the MIZEX campaign in the 1980s (Squire & Montiel 2016), suggest that the physics is well understood compared to other topics in wave–ice interaction.

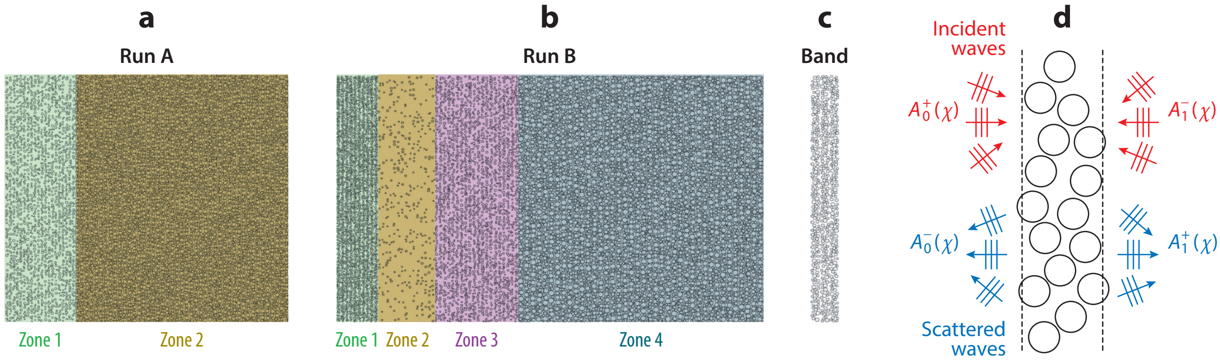

Figure 3

(*a–c*) Examples of strip structures from real marginal ice zones (MIZs). (*d*) Mapping between incident (*red*) and scattered (*blue*) waves across a single strip. The incident wave directional spectrum $A_0^+(\chi)$ (*red*) enters the first strip at the ice edge from open sea to the left, where it is scattered by floes inside the strip. The reflected spectrum is labeled $A_0^-(\chi)$ (*blue*), while the spectrum transmitted into the next strip is labeled $A_1^+(\chi)$ (*blue*). The second strip transmits wave energy to the right but also reflects energy with a directional spectrum $A_1^-(\chi)$ (*red*) back into the first strip. The same behavior occurs at successive contiguous strips farther into the interior of the MIZ. Directionality is encapsulated in the quantity χ. Figure adapted with permission from Squire & Montiel (2016).

The scattering kernel $K(\theta - \theta')$ that appears in Equation 2 is required to apply the results of this section to ESMs, ice/ocean models, and WW3, but it is not obvious how to find it. By computing the spectrum of the linear operator defined by Equation 2 under a particular nondimensionalization, Meylan & Bennetts (2018) found that the spectrum has a universal structure and, consequently, that wave scattering in the MIZ has similar properties for a large range of ice types and wave periods. The method facilitates computation of the spatial and temporal evolution of wave packets transiting the MIZ, i.e., how they attenuate and spread with distance traveled. For 100-m-diameter ice floes, the 8-s wave packet eventually becomes directionally isotropic as it proceeds deeper into the MIZ, accordant with other studies (e.g., Montiel et al. 2016, Squire & Montiel 2016, Boutin et al. 2018).

2.2. Pancake Ice, Frazil, and Grease Ice

As the ocean water begins to freeze, tiny needle-like ice crystals called frazil form, which accumulate and bond together at the sea surface to give it a greasy appearance. Grease ice, as it is called, can develop into nilas if the seas are calm and eventually grows into a more stable ice sheet, which gradually thickens. When the seas are rough, however, the frazil crystals accumulate into slushy circular disks, called pancakes because of their shape. Ice pancakes have raised edges or ridges on their perimeters, caused by the pancakes bumping into each other under the action of the ocean waves. If the motion is strong enough, the pancakes can raft over one another to create an uneven top and bottom surface. Eventually, the pancakes cement together and consolidate into a coherent ice sheet. Once sea ice forms into sheet ice, it continues to grow through the winter. Grease ice can also be herded and piled up, for example, at the edges of polynyas under the action of strong katabatic winds that descend from elevated terrestrial ice sheets.

In this section, we focus on ice covers that have not consolidated into solid ice, i.e., primarily suspensions of pancake and grease ice. This type of sea ice is seen over vast areas of the outer reaches of the Southern Ocean MIZ in midwinter (Wadhams et al. 1987), but as discussed by Thomson et al. (2018), extensive pancake ice formation is also now being observed in the western Arctic because of the increasingly energetic wave climate there. As contended earlier, because pancake ice, frazil, and grease ice have length scales much smaller than typical ocean wavelengths, viscous dissipation in the ice slurry overshadows any attenuation arising because of scattering.

2.2.1. The viscoelastic model of Wang & Shen (2010). Wang & Shen (2010) generalized earlier models of ice-coupled wave propagation in continuous ice (e.g., Fox & Squire 1994, Keller 1998) by representing the ice–ocean system as a homogeneous viscoelastic fluid layer of finite thickness overlying an inviscid layer of finite depth (see also Zhao et al. 2015). Viscoelasticity is accounted for by a Voigt constitutive equation, identified by a complex modulus involving a shear modulus G and a viscosity ν. Viscosity is proposed to originate from the frazil ice or ice floes much smaller than the wavelength, while elasticity arises from ice floes that are relatively large compared to the wavelength. Since the lower layer is inviscid, its velocity field can be represented by a velocity potential, while the upper layer is configured in terms of a velocity potential and a stream function. (As a result, the model is constrained to be 2D.) The model assumes continuity of the normal stress and shear stress at the upper free surface, where both vanish, and at the lower surface, i.e., the interface between the two fluids. Noting that the quantities do not have to be in phase, the Airy wave mode ansatzes of Section 1.2 for the vertical displacements at the free surface and at the interface prescribe the format of the velocity potentials and stream function and allow the dispersion relation to be written down. While complicated, the full dispersion relation reduces to versions published earlier, namely, those of the mass loading model, the thin elastic plate model, and the viscous layer model for simplified constitutive equations (Squire 2007). However, the full dispersion relation has multiple roots (Zhao et al. 2017) that can lie very close together in the complex plane, making it challenging to track roots as G and ν move in parameter space. This forced Wang & Shen (2010) to introduce criteria to select the primary propagating wave mode, i.e., (*a*) the wave number closest to the open water value and (*b*) the attenuation rate least among all modes. By investigating several simpler models, Mosig et al. (2015) reproduced many of the subtleties reported by Wang & Shen (2010) without the jumping between wave modes that occurs as G and ν transit parameter space. Furthermore, due to the requirement of empirically fitting the sea ice rheology, the Wang & Shen (2010) viscoelastic model also has an extra degree of freedom for fitting and thus provides improved consistency with observations irrespective of whether the physics is correct. Nonetheless, for homogeneous pancake ice slurries, it is a rational progression from preceding models.

Ancillary analyses were conducted by Wang & Shen (2011) to describe approximately how a wave train would change as it crossed the junction between open water and ice cover defined by the Wang & Shen (2010) dispersion relation, and across strips of ice cover with different material constants (Zhao & Shen 2013). Because of the complexity of the Wang & Shen (2010) dispersion relation, matching the full set of wave modes across these junctions has never been achieved, notwithstanding the variational model of Zhao & Shen (2015a) based upon a simpler elastic investigation (Fox & Squire 1994), which shows errors associated with the approximation to be acceptable in most cases. In order to understand the sensitivity of the Wang & Shen (2010) model to variations of its free parameters (namely, wave frequency, water depth, ice thickness, G, and ν), Li et al. (2015b) applied ANOVA (analysis of variance) to the viscoelastic dispersion relation using a stratified Monte Carlo simulation. The aim was to assess the implications of the model's behavior on inversely determining the model parameters. They also compared these results with those of an early discarded 1980s model (Squire & Allan 1980), which presented an analogous dispersion relation for a Kelvin–Voigt viscoelastic thin plate. The results were qualitatively the same, but the strong interactions that occur between physical parameters affirmed that wave period and ice thickness must be accurately measured to inversely determine G and ν. Although the analysis of Li et al. (2015b) was statistically based, it connected strongly to the deterministic study by Mosig et al. (2015), which considered another type of floating viscoelastic thin plate. Under controllable laboratory conditions, Zhao & Shen (2015b) used a least square fitting method that inversely determined G and ν at different values of f in a set of experiments on pancake ice, a mixture of frazil and pancake ice, and fragmented ice. The viscoelastic model did a reasonable job fitting the observations in each case.

2.2.2. Viscoelastic extensions and alternatives. Zhao & Shen (2018) have extended the two-layer model of Wang & Shen (2010) to three layers—a homogeneous viscoelastic layer defined by (G, ν) representing ice above a viscous water layer of finite thickness, which is over an inviscid layer of finite depth. The extra intermediate viscous layer is intended to mimic a turbulent boundary layer identified by an eddy viscosity, which is explored after first validating the model against known simpler solutions.

Like Wang & Shen (2010), De Santi & Olla (2017) sought to expand the viscous layer model of Keller (1998), but they did so by cleverly adding a fictitious layer of infinitesimal thickness, where the pancakes are confined, which modifies the contribution to the stress at the upper ice surface. Macroscopic equations were found by ensemble-averaging the fluid equations at the pancake scale in the asymptotic limit of long waves and low pancake surface fraction, thereby producing a dilute theory with no interactions. De Santi & Olla (2017) also carried out a semiquantitative close-packing (CP) analysis that is more suited to pancake ice and predicted a damping larger than that obtained by Wang & Shen (2010). De Santi et al. (2018) tested the CP model against field data from the Arctic and the Antarctic, along with two other models. Each model performed well (see **Figure 4**), but the CP model fitted field data for values of the ice viscosity comparable to those of grease ice obtained in laboratory experiments, while for the simpler Keller (1998) viscous layer model that omitted the important contribution made to damping by pancakes, unrealistic values of viscosity were necessary when the ice was thick. By fixing the viscosity, the CP model also gave best fit instance-by-instance ice thickness values that were close to observations and more stable than the Keller (1998) model.

Recognizing the substantial vertical gradients that commonly prevail in floating sea ice, G. Sutherland et al. (2018) deftly parameterized the ice itself as a two-layer structure, assuming an oscillating pressure gradient in an upper impermeable layer and acknowledging that the remainder of the sea ice is too viscous to be considered solid over the temporal scales of typical ocean waves. The viscosity was derived using dimensional analysis.

3. OBSERVATIONS AND EXPERIMENTS

3.1. Laboratory Studies

Although experiments done in wave flumes or wave basins can be very helpful in gaining an understanding of how waves and ice floes interact, especially because of the controllable environment in which they are conducted, they do have their limitations. For instance, no facility can replicate nature in regard to size, so experiments are constrained to short wavelengths; most operate at room temperature so real ice cannot be used; the material properties of sea ice are dependent on strain rate and difficult to replicate with alternatives such as plastics; scaling up results is problematical; and so on. If laboratory-grown sea ice can be accommodated, e.g., at HSVA (Hamburgische Schiffbau-Versuchsanstalt GmbH), it may behave profoundly differently mechanically from natural sea ice under wave action because of the complex physical structure of sea ice in situ. Nevertheless, considerable insights can be gained from the laboratory at modest cost compared to ship-based field programs.

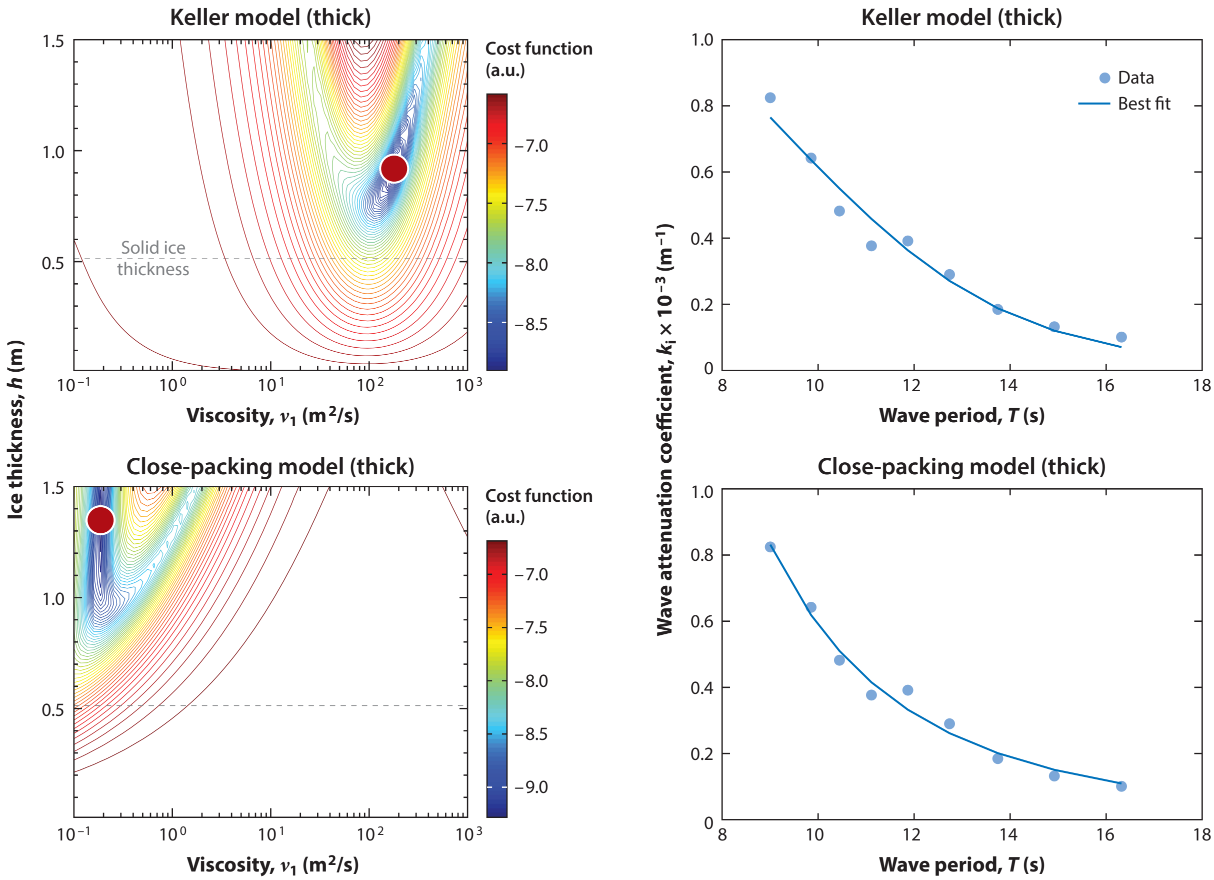

Figure 4

Fit of Weddell Sea data for a thick ice layer, collected at 3:00 AM on April 26, 2000, during the ANT-XVII/3 cruise leg of the R/V Polarstern. The left plots show contours of the cost function in arbitrary units used to find the best fit (*red dots*) to data, with the measured equivalent solid ice thickness shown as a dotted line, and the right plots show best fits (*blue lines*) to observed wave amplitude coefficient k_i data (*blue circles*). (*Top plots*) Keller (1998) model; (*bottom plots*) De Santi & Olla (2017) close-packing model. Figure adapted with permission from De Santi et al. (2018).

3.1.1. Solitary floating plates. Laboratory experiments of wave–ice interaction are normally limited to simple plate geometries such as squares (Bennetts et al. 2015a, Meylan et al. 2015a) or circular discs (Montiel et al. 2013a,b; Meylan et al. 2015b) manufactured from stiff or compliant plastics of different thicknesses with similar densities to ice. By minimizing undesirable artifacts in the wave tank, e.g., reflections from the tank's walls, the simplest experiments can measure the deformation of the floating plate at several wave periods and for gentle to sizable wave slopes and then compare these data with a model. The diffracted wave field can also be studied either from single plates or a few interacting ones. Depending on the desired outcomes, the plates can be horizontally constrained or allowed to move freely with the wave and drift, and overwashing can be prevented or investigated. Meylan et al. (2015a) assembled a theoretical model that reproduced well the bending of 1-m-square plastic plates subjected to modest waves in a wave basin, particularly for the thinner of the 5-mm and 10-mm sheets tested. Interestingly, nonlinear wave–plate interaction phenomena, in particular overwash but also slamming, drift, and (linear) surging, only had a negligible effect on the floating plate's flexural motions. In contrast, Bennetts et al. (2015a) found that waves transmitted by the plate are regular for gently sloping incident waves but irregular for storm-like incident waves, with the proportion of the incident wave transmitted decreasing as incident wave steepness increases to be at its minimum for an incident wavelength equal to the floe length. This was attributed, in part, to wave energy dissipation caused by wave overwash of the floe and slamming of the floe against the water surface, both of which become stronger as the incident waves become steeper.

Toffoli et al. (2015) conducted a superficially straightforward experiment using a thin plastic sheet in a wave flume to determine whether what they call "the solitary floe version of the quintessential theoretical model of wave attenuation" (p. 7) could be validated. They found that the theoretical model predicted transmitted wave amplitudes accurately for gently sloping incident waves ($ka \leq 0.06$), where a is the wave amplitude, i.e., half the (peak-to-trough) wave height, but it increasingly overpredicted transmitted amplitudes as the incident waves became steeper and increasingly storm-like. The loss of agreement was shown to correlate with the wave energy being dissipated. An extended analysis (Nelli et al. 2017) contends that overwash and drift affect reflection and transmission for $ka \geq 0.08$, implying that the Airy linear ansatz defined in Section 1.2 may be suitable to model wave attenuation only for relatively mild incident waves. While this may be true, and while acknowledging the trend toward greater wave heights that we are experiencing due to global climate change, e.g., in the western Arctic (Young et al. 2011, Liu et al. 2016, Thomson et al. 2018), we must also recall that waves are attenuated rapidly by sea ice in nature, so linear theory may hold within the interior of the MIZ while, within the ice edge zone, overwash and other nonlinear effects will be pervasive (see, e.g., Squire & Moore 1980).

Yiew et al. (2016, 2017) conducted experiments on floating discs in the manner of Montiel et al. (2013a,b) but focused particularly on the surge (see also Meylan et al. 2015b), heave, and pitch motion induced by regular incident waves. Two to three incident steepnesses were considered for each frequency, and four to six steepnesses were considered for two frequencies to test the steepness dependence in two different wavelength regimes. Results were compared to two models, slope-sliding theory and a potential flow model that represents the disc as a thin plate. The latter model compares favorably with data but could be improved at shorter wavelengths by including the effects of overwash (Skene et al. 2015). Yiew et al. (2017) studied collisions between two thin floating discs arising from regular water waves in a laboratory wave basin, analyzed using slope sliding theory. The agreement between model and data implies that the model could act as a basis for modeling nonrafting collisions due to waves in a MIZ.

I have already mentioned some experiments done at HSVA by Zhao & Shen (2015b) to parameterize the Wang & Shen (2010) viscoelastic ice layer model using a least squares architecture. I also mention the investigation by Dolatshah et al. (2018), which started with an ice sheet grown in a wave flume and aimed to discover if or when the ice sheet will break when subjected to regular waves. Dolatshah et al. (2018) found that only incident waves with sufficiently long period and large steepness fracture the ice cover and that the extent of breakup increases as period and steepness increase. It is unclear whether the beach at the far end of the flume works when it is ice covered, but the paper is interesting regardless. However, the statement "The results [show], for the first time, simultaneous observations of wave propagation and wave-induced ice breakup" (p. 4) is incorrect, as wave-induced ice breakup has been observed on several occasions, and in fact, a video has even been made of the process by Dr. Dany Dumont at the Université du Québec à Rimouski (**https://www.ismer.ca/recherche/equipe/dumont-dany**).

3.1.2. Transmission through many floating discs. Although some early laboratory experiments were done to quantify the behavior of surface waves as they propagate through an array of floating discs, e.g., by Emeritus Professor Peter Wadhams during his PhD, to my knowledge, recent work is limited to the study by Bennetts & Williams (2015), who used approximately 1-m-diameter × 33-mm-thick wooden discs at low and at high concentration floating in a wave basin. Two models that independently predict a similar monotonic increase in transmission as wave period increases were compared with the data sets, a 2D scattering model and a transport model. Results indicated that the models predict wave energy transmission accurately for small-amplitude waves and low-concentration arrays; the high-concentration array transmits less energy than the low-concentration array. Discrepancies for large-amplitude waves and high-concentration arrays were attributed to wave overwash of the discs and collisions between discs. For the low-concentration array and small-amplitude waves, the agreement between the models and data indicate that in this regime (*a*) the redistribution of wave energy due to scattering is the dominant contributor to the measured wave attenuation and (*b*) linear thin plate/potential theory and transport theory provide a valid model to determine wave transmission through an array of floating discs.

3.2. Wave–Ice Interaction Fieldwork

In their overview of the Arctic Sea State program in a special section of *Journal of Geophysical Research Oceans*, Thomson et al. (2018) explained how the Arctic is shifting to a more seasonal system, where a dramatic increase in open water extent and duration in the autumn means that large surface waves and significant surface heat fluxes are now common. An in situ field campaign associated with the program took place throughout a cruise aboard the ship R/V Sikuliaq in the Beaufort Sea over 42 days during the boreal autumn of 2015. A concentration on the specific role of surface waves and winds in the new Arctic, with a focus on the autumn refreezing period—supported by aerial (NASA and Naval Research Laboratory) and satellite (RADARSAT-2 and TerraSAR-X) remote sensing and modern surface instrument technologies—and a strong emphasis on using and improving forecasting models, provides a hitherto unrivalled, comprehensive data set to validate and potentially calibrate theoretical advances. Uniquely, wave experiments took precedence aboard the Sikuliaq whenever there was a favorable forecast for waves, with other research conducted around these events.

3.2.1. The 2015 Beaufort Sea field campaign. Commenting holistically on the Beaufort Sea cruise, Thomson et al. (2018) mentioned the predominance of pancake ice near the ice edge, which is quite novel for the western Arctic and arises as a direct consequence of increasing wave activity. Under calmer conditions nilas formed. These are crucial observations that undergird consequential analyses of the data set to extract information for modeling or forecasting purposes, such as how the waves attenuate and collimate or spread, because the average diameter of sea ice pancakes is much smaller than typical ocean wavelengths, so scattering is not expected to be important, i.e., α_{scat} is much less than α_{dis}. This was confirmed by Cheng et al. (2017), who showed that elasticity, expressed through G, is less important than the viscous damping ν in the ice layer in this regime by using the full suite of wave observations in pancake ice to determine attenuation and then calibrated the viscoelastic model of Wang & Shen (2010) encoded through the so-called WW3 IC3 module representing S_{ice} in Equation 1. Unfortunately, even though seven independent wave experiments were done using freely drifting buoys, the resulting calibrated viscoelastic parameters can only be used in WW3 for wave forecasts where pancake ice dominates. Should pancake ice become as prevalent in the Arctic MIZ as it is in Antarctica, opportunities exist to refine these parameters. Helpful in this respect are the energy attenuation coefficients calculated by Doble et al. (2015) from in situ data transmitted by buoys deployed into the advancing pancake ice region of

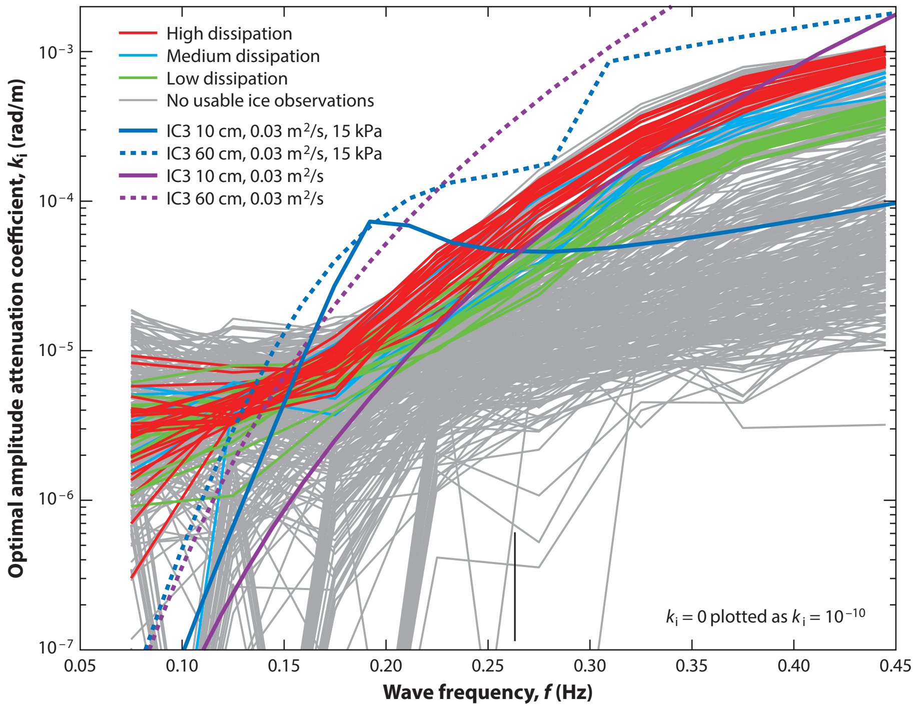

Figure 5

Optimal amplitude attenuation coefficient, k_i, plotted as a function of wave frequency, f. Dissipation profiles from a simple application of the Wang & Shen (2010) model are shown without elasticity (*purple lines*) and with elasticity (*blue lines*), each found by inversion for two ice thicknesses, alongside field data from the 2015 R/V Sikuliaq Beaufort Sea cruise. Figure adapted with permission from Rogers et al. (2016).

the Weddell Sea, Antarctica, during temporally and spatially fluctuating ice conditions. Attenuation varied by more than two orders of magnitude and was far higher than that observed in MIZs composed of solid ice floes—significant wave height decreased from up to 3.7 m with mean periods down to 5 s at the outer buoy, to 1.1 m at the middle buoy where the mean period minimum was 8 s, and to insignificant wave energy at the innermost buoy. The Doble et al. (2015) data set suggests an approximate squared relation between α_{dis} and frequency f and a linear relation with the equivalent (solid) pancake ice thickness h_{eq}, namely, $\alpha_{\mathrm{dis}} \propto h_{\mathrm{eq}} f^2$. Subsequently, Meylan et al. (2018) have associated f^2 behavior of the attenuation coefficient with energy loss arising from the product of the fluid pressure and velocity, which is plausible for pancake ice.

Rogers et al. (2016) created a hindcast of a particular wave event that occurred during the Beaufort Sea cruise by applying WW3 with the Wang & Shen (2010) IC3 S_{dis} module to analyze and interpret extensive buoy and shipborne measurements of wave spectra. Recalling that the energy attenuation coefficient is twice that for amplitude, namely, k_i, **Figure 5** shows k_i plotted against f from 403 wave buoy spectra collected during the 2015 field experiment in a mixture of pancake ice and frazil. Evidently, the fitted curves are steeper than indicated by data, and although elasticity reduces the steepness, there is also a suggestion in the figure that the introduction of elasticity increases instability due to jumps between wave modes during inversion (see Section 2.2 above and Mosig et al. 2015). In their analysis of dispersion relations in the limit of thin ice, weak attenuation, and waves that disperse as in open water, Meylan et al. (2018) did not include the

Significant wave height: mean wave height (trough to crest) of the highest third of the waves, nowadays defined as four times the standard deviation of the surface elevation

Wang & Shen (2010) model because of its complexity. However, it is reasonable to expect that a high power of n in $k_i(f) \propto f^n$ contributes to the observed steepness.

Montiel et al. (2018) selected a specific experiment from the Beaufort Sea cruise, conducted using 11 wave-measuring buoys tracked for three days during a storm event from October 11 to 14, 2015. Both attenuation and directional aspects of the wave field in the sea ice were analyzed, but severe icing caused various problems that led to differences between the two types of buoy deployed. Useful information about the decay of significant wave height and spectral amplitude metrics was nevertheless extracted, and the energy decay satisfied $\alpha_{\mathrm{dis}} \propto f^{2.2}$, i.e., was close to the f^2 relationship found by Doble et al. (2015) for Antarctic pancake ice. Although the decay of spectral amplitudes remains predominantly exponential for the range of values observed during the wave event, positive correlations occurred for one of the two wave buoy types with linear decay when the wave height was large. It remains to be seen whether this is a robust interpretation, but if it is, it suggests that the Airy ansatz of Section 1.2 may not always hold and alternative models such as that proposed by Squire (2018) might be considered. Interestingly, in a recent laboratory experiment that examined the enhanced damping of surface waves by floating spherical particles, Sutherland & Balmforth (2019) found exponential decay in time when no particles were present but exponential decay followed by power law decay after lower amplitudes had been reached, due to flows between particles and flows forced through particles by expanding and contracting particle separations. In the October Beaufort Sea experiment, both frequency-averaged and frequency-resolved metrics of the directional spread decreased with distance of propagation into the pancake ice, i.e., the wave field became more collimated. Wave dispersion during the same experiment was analyzed by Collins et al. (2018), who concluded that waves dispersed as though in open water for $f \leq 0.30\,\mathrm{Hz}$ but that a small increase in wave number compared to that expected in open water is seen for $f > 0.30\,\mathrm{Hz}$.

3.2.2. Cognate in situ studies. Other valuable but less exhaustive fieldwork of relevance has been conducted, e.g., in the Antarctic MIZ during September–October 2012 when five wave sensors were tracked (Kohout et al. 2014, Meylan et al. 2014); experiments in the waters off Svalbard, where attenuation was recorded in continuous and broken pack ice [Collins et al. (2015), modeled by Boutin et al. (2018)], landfast ice (Sutherland & Rabault 2016), and grease ice (Rabault et al. 2017); and the recently completed PIPERS (Polynyas, Ice Production, and Seasonal Evolution in the Ross Sea) experiments in the winter Ross Sea, which included wave buoy measurements. In sum, these and other, earlier complementary investigations (e.g., Squire & Moore 1980; Wadhams et al. 1986, 1987; Wadhams & Doble 2009) contribute incrementally to our depth of understanding of how ocean waves are affected by the many variations of sea ice that exist in nature and, conversely, how that ice is modified by the potentially destructive waves.

3.2.3. Remote sensing. The development of quantitative models describing wave–ice interaction demands a parallel stream of investigation that tests, calibrates, and tunes those models in situ, i.e., in the polar and subpolar seas. Laboratory studies can certainly assist, but as noted earlier in Section 3.1, they have drawbacks that make direct application of outcomes challenging. Yet, while enjoyable in moderate doses, fieldwork in the Arctic and Antarctic is rarely a low-cost endeavor, and monitoring ocean waves during their passage through heterogeneous fields of sea ice is perversely difficult even if nature provides the waves in the first place (which it does not always do). Sea ice is notoriously variable spatially and temporally, so no matter how good the experimental design is and how state-of-the-art the instruments deployed are, the data set obtained only represents a short-term visualization of a continuously changing natural process.

Utilizing both satellites and aircraft missions, remote sensing has consistently provided valuable data sets that can complement or, in some instances, even replace field observations done in situ. Acknowledging that some vital measurements remain elusive, technology has advanced to the point where remote sensing is set to become the pervasive future data source for testing models of ocean waves passing into and through sea ice fields, supported by in situ surface validation and well-instrumented drifting buoys that communicate their data streams by satellite.

SAR: synthetic aperture radar

Wind and wave parameters can be readily derived from synthetic aperture radar (SAR) data in the open water and wave heights, and remarkably, full spectra can now also be recovered in ice-covered regions (Ardhuin et al. 2015, 2016, 2017, 2019). That method of wave spectra retrieval in ice-covered water was adapted by Stopa et al. (2018a) to handle a mixture of wave and ice features, producing the first map of wave heights extending over 400 km into the sea ice field, and to estimate the azimuthal cutoff needed to correct for the blurring of wave patterns near the ice edge. Shen et al. (2018) presented an interrelated study of wave–ice interactions in the MIZ off southeast Greenland, which retrieved wave information about dispersion, attenuation, and directional adjustments from the polarimetric RADARSAT-2 SAR that is consistent with model simulations and field observations. Valuable estimates of MIZ waves over large spatial scales at high resolution are provided by the SAR measurements. Using wave height estimations from SAR imagery performed up to 400 km into the ice, the three-day October Beaufort Sea experiment described and interpreted by Montiel et al. (2018) was also selected by Ardhuin et al. (2018) to evaluate the parameterizations presented by Boutin et al. (2018) for scattering by ice floes, basal friction, inelastic dissipation due to dislocations in the ice, and ice breakup. Ardhuin et al. (2018) inferred that dissipative mechanisms dominate for thin pancake ice at the observed periods around 10 s and that scattering has a weaker effect on wave heights.

Although the discussion above has focused on satellite remote sensing and especially SAR, aircraft remote sensing is also an immensely valuable tool for studying waves penetrating fields of sea ice. An example of this is the informative paper by P. Sutherland et al. (2018), which uses scanning lidar to produce high-quality estimates of directional wave number spectra in the MIZ for 234 independent 2-km flight segments extending from approximately 15 km inside the ice edge to 55 km outside it during the Beaufort Sea campaign.

3.3. Other Notable Experiments

In this section, I highlight three studies of wave–ice interactions that I consider particularly insightful (Li et al. 2017, Roach et al. 2018, Wadhams et al. 2018).

Li et al. (2017) investigated a long-standing (four decades) conundrum of wave–ice interaction data that defies all of the models, namely, that attenuation does not increase monotonically as frequency increases but instead rolls over at a particular frequency and decreases. Many modelers would say that there is something wrong with the data, but using WW3 and recent data from two independent and very different field experiments in the Antarctic MIZ, Li et al. (2017) attributed the discrepancy between data and models to wind input and nonlinear transfer of wave energy between different wave frequencies. This has the effect of offsetting the damping caused by the sea ice and results in the apparent reduction of attenuation at high frequencies.

Roach et al. (2018) applied image processing to images of pancake ice at various stages of growth obtained by drifting wave buoys during the 2015 Beaufort Sea campaign. The diameters of pancake ice floes, which mature from pancakes initially formed in freezing, low-wave conditions, were found to be limited by the wave field such that floe diameter was proportional to wavelength and amplitude over time. Understanding how floes grow laterally and weld will allow new models that evolve sea ice FSD to be developed.

In Section 2.1.1 we alluded to a method to determine ice thickness remotely using ice-coupled waves (Williams & Squire 2010), recognizing that although satellite sensors have shown recent promise, thickness remains especially difficult to measure directly from space. Applying ideas formulated in an earlier paper (Wadhams & Holt 1991) to the Beaufort Sea data set, Wadhams et al. (2018) tested and applied a method for measuring thickness using SAR images of ocean waves dispersing in pancake ice, observed by high-resolution instruments aboard the Sentinel-1 and COSMO-SkyMed satellites. Summarizing a very thorough analysis, the authors used the viscous layer model of Keller (1998), which accounts for wave dispersion and attenuation as functions of wave number and ice properties for the pancake ice subscenes, to invert the SAR spectra and compute, parametrically, the pancake ice thickness and the wave attenuation rate. They reported that the thickness estimation technique works well and yields credible thickness values combined with consistent values for kinematic viscosity (0.03–0.05 m^2/s).

Sentinel-1: the first of the Copernicus Programme satellite constellation conducted by the European Space Agency

CICE: the Community Ice Code, a computer model for the growth, melting, and movement of polar sea ice; officially named the Los Alamos Sea Ice Model

4. EARTH SYSTEM MODELS AND WAVE FORECASTING MODELS

At the start of this review I listed the four goals of the Arctic Sea State program as documented by Thomson et al. (2018). The final goal, "applying the results [of the program] in coupled forecast models" (Thomson et al. 2018, p. 8675) has received considerable attention during the program with regard to WW3 (WW3DG 2016), as corroborated by **Table 1**. At the start of the program, only IC0 existed, which is a very poor representation of what happens to ocean waves as they penetrate fields of sea ice. While appreciable variations remain between the predictions of the IC schemes (dissipation modules), and while the IS schemes (scattering modules) are at an early stage of development, considerable progress continues to be made as better modules are fine-tuned for different sea ice types and developed to parameterize wave–ice interactions.

Progress has also been made with regard to ESMs, although direct outcomes from the Arctic Sea State program are currently less well advanced in this respect. Before and at the start of the program, Dumont et al. (2011) and Williams et al. (2013a,b) reported early models that embedded waves into ice/ocean models, and more recently Williams et al. (2017) described an entirely new sea ice model called neXtSIM based on an elasto-brittle rheology, which accommodates wave–ice interactions. Wave radiation stress was a major point of interest of Williams et al. (2017) and Stopa et al. (2018b). The consequences of wave-induced breakup of Antarctic sea ice in the archetypal CICE (Community Ice Code) sea ice model were investigated by Bennetts et al. (2017), who had earlier published their thoughts on constructing wave–ice interaction models in the context of large-scale ESMs (Bennetts et al. 2015b).

Table 1 Wave–ice interaction schemes in WAVEWATCH III®

Scheme	Mechanism(s)
IC0	Partial blocking, scaled by ice concentration; high concentration treated as land
IS1	Simple conservative diffusive scattering term
IS2	Floe size–dependent conservative scattering, combined with ice breakup and anelastic or inelastic dissipation due to ice flexure
IC1	Simple dissipation, uniform in frequency
IC2	Basal friction, laminar or turbulent
IC3	Ice as viscoelastic layer (Wang & Shen 2010), frequency-dependent
IC4	Assorted parametric and empirical formulas, most being frequency-dependent
IC5	Ice as viscoelastic layer [extended from Fox & Squire (1994)], frequency-dependent

IC schemes designate dissipation modules, and IS schemes designate scattering modules. Table adapted from Thomson et al. (2018).

5. CONCLUSION

Before concluding with some personal reflections germane to current wave–ice interaction research, I mention another facet of the topic that is not explored in this review, which has been focused entirely on sea ice as opposed to other kinds of floating ice. Since 1995, three large ice shelves on the Antarctic Peninsula—the Larsen A, Larsen B, and Wilkins—have suddenly and dramatically disintegrated. Massom et al. (2018) discovered that when Antarctica's massive ice shelves lack a protective buffer of sea ice, ocean swells from the north flex the ice shelves and can weaken their stabilizing seaward edge and thereby hasten their disintegration into icebergs. Because ice shelves slow the flow of ice from the massive Antarctic ice sheet, rapidly disintegrating shelves have troubling implications for sea level rise.

Ice shelf: the portion of a terrestrial ice sheet that spreads out over water, formed where tributary glaciers and ice sheets flow into the sea

IPCC: Intergovernmental Panel on Climate Change

Prompted by the uncompromising effects of global climate change on the polar seas, there has been a staggering resurgence of interest in how ocean wave trains are affected by ice fields of various kinds and how the sea ice that constitutes those ice fields is altered by the waves. Arctic sea ice, especially, has metamorphosed physically over the last twenty years or so to be more like that of the Antarctic, and it continues to change, with the IPCC (Intergovernmental Panel on Climate Change) Fifth Assessment Report making dire predictions of an ice-free summer just decades away (**https://www.ipcc.ch/report/ar5/syr/**). Changes to storminess in a warming world, alongside substantially increased fetches for waves to develop and intensify, will alter the physiology of the sea ice and facilitate greater wave-induced breakup. The sea ice around Antarctica is also subjected to prolonged intensive ocean wave activity, arising because of the vast fetches to the north. While the extent and thickness of sea ice there have not yet changed significantly due to the differences in geography, ocean properties, and atmospheric circulation between the Antarctic and Arctic, ocean waves will also always be contributing factors that regulate sea ice morphology in the Southern Ocean.

A simple power law of modest order (2–4) appears repeatedly in data that describe how the attenuation coefficient varies with frequency, and this applies over a range of different ice conditions. Meylan et al. (2018) presented results from four independent field experiments to illustrate this, and under the assumptions of thin ice, weak attenuation, and waves that disperse as in open water, they investigated three commonly used dispersion relations. Two of these introduce viscosity into a simple elastic thin plate, either by subsuming simple frictional viscous damping or by making the elastic modulus complex (cf. Wang & Shen 2010), and the third is a pure viscous layer model (Keller 1998). While simple frictional damping produces a power index between 2 and 4, the other two dispersion relations are way off; hence, Meylan et al. (2018) went on to try other physical mechanisms that might lead to $k_{\mathrm{i}} \propto f^n$ for n in the 2–4 range. It is crucially important that future IC dissipation parameterizations in WW3 accommodate suitable power law behavior, as the ones listed in **Table 1** do not (see also **Figure 2**).

Better parameterizations are needed for all physical processes in ESMs, ice/ocean models, and wave forecasting systems such as WW3. Our comprehension of the physics of wave–ice interactions is patchy; for example, we do not yet have a persuasive parameterization for how waves dissipate in a slurry of pancake ice and frazil that captures the physics of the attenuation. I am excited by the work of De Santi & Olla (2017) and De Santi et al. (2018) in this regard, but more work clearly needs to be done. For a MIZ composed of separate ice floes, we can compute α_{scat} reasonably effectively, but again we have less confidence modeling α_{dis} because the floe fluid physics is nonlinear. Heterogeneity and nonstationarity of the ice field and waves create further challenges. While less satisfying, empirically based parameterizations grounded in field data may be the solution, recognizing the apparent pervasiveness of the power law $k_{\mathrm{i}} \propto f^n$ discussed above.

The dispersion relation that arises from the Kirchhoff–Love thin elastic plate [as used by, e.g., Fox & Squire (1994) and many others] and the viscous layer model of Keller (1998) are both comparatively straightforward, while the aesthetically satisfying mathematical generalization outlined by Wang & Shen (2010) turns out to have complicated and unhelpful repercussions in terms of the configuration of the infinity of wave modes in the complex plane as G and ν vary in parameter space. When G and ν are known, this is not a problem, but it is troublesome when no a priori information is available about G and ν and they are being sought from data that may not fit the model in the first place [see Meylan et al. (2018) and again the discussion above], as G and ν will often be physically meaningless (Mosig et al. 2015). Furthermore, G and ν represent the MIZ at only one point in time and at one location.

While it is essential that the validation of theory and models continues, it should evolve to focus largely on remote sensing and remotely tracked buoys, with surface truth, so that the intrinsic temporal and spatial variability of data sets can be circumvented.

DISCLOSURE STATEMENT

The author is not aware of any biases that might be perceived as affecting the objectivity of this review.

ACKNOWLEDGMENTS

I am grateful to the Office of Naval Research (ONR) and especially Drs. Martin Jeffries and Scott Harper, who masterminded and funded the Arctic Sea State departmental research initiative at a seminal time in polar marine science. I thank the many colleagues and friends who were involved in the program and acknowledge support from ONR (award N00014-131-0279), EU FP7 Grant (SPA-2013.1.1-06), the University of Otago, and the Isaac Newton Institute for Mathematical Sciences (EPSRC grant number EP/K032208/1), which awarded me a Simons Fellowship that helped me prepare this timely reappraisal of the field, mindful of the effects of global climate change. Thanks also to the many graduate students and postdoctoral fellows I have enjoyed working with during my career.

LITERATURE CITED

Ardhuin F, Boutin G, Stopa JE, Girard-Ardhuin F, Melsheimer C, et al. 2018. Wave attenuation through an Arctic marginal ice zone on 12 October 2015: 2. Numerical modeling of waves and associated ice breakup. *J. Geophys. Res. Oceans* 123:5652–68

Ardhuin F, Collard F, Chapron B, Girard-Ardhuin F, Guitton G, et al. 2015. Estimates of ocean wave heights and attenuation in sea ice using the SAR wave mode on Sentinel-1A. *Geophys. Res. Lett.* 42:2317–25

Ardhuin F, Stopa JE, Chapron B, Collard F, Jensen RE, et al. 2019. Observing sea states. *Front. Mar. Sci.* 6:124

Ardhuin F, Stopa JE, Chapron B, Collard F, Smith M, et al. 2017. Measuring ocean waves in sea ice using SAR imagery: a quasi-deterministic approach evaluated with Sentinel-1 and in situ data. *Remote Sens. Environ.* 189:211–22

Ardhuin F, Sutherland P, Doble MJ, Wadhams P. 2016. Ocean waves across the Arctic: Attenuation due to dissipation dominates over scattering for periods longer than 19 s. *Geophys. Res. Lett.* 43:5775–83

Bennetts LG, Alberello A, Meylan MH, Cavaliere C, Babanin AV, Toffoli A. 2015a. An idealised experimental model of ocean surface wave transmission by an ice floe. *Ocean Model.* 96:85–92

Bennetts LG, Biggs NRT, Porter D. 2007. A multi-mode approximation to wave scattering by ice sheets of varying thickness. *J. Fluid Mech.* 579:413–43

Bennetts LG, Biggs NRT, Porter D. 2009. The interaction of flexural-gravity waves with periodic geometries. *Wave Motion* 46:57–73

Bennetts LG, O'Farrell S, Uotila P. 2017. Brief communication: impacts of ocean-wave-induced breakup of Antarctic sea ice via thermodynamics in a stand-alone version of the CICE sea-ice model. *Cryosphere* 11:1035–40

Bennetts LG, O'Farrell S, Uotila P, Squire VA. 2015b. An idealized wave–ice interaction model without subgrid spatial or temporal discretizations. *Ann. Glaciol.* 56:258–62

Bennetts LG, Peter MA, Squire VA, Meylan MH. 2010. A three-dimensional model of wave attenuation in the marginal ice zone. *J. Geophys. Res. Oceans* 115:C12043

Bennetts LG, Squire VA. 2009. Wave scattering by multiple rows of circular ice floes. *J. Fluid Mech.* 639:213–38

Bennetts LG, Squire VA. 2012a. Model sensitivity analysis of scattering-induced attenuation of ice-coupled waves. *Ocean Model.* 45-46:1–13

Bennetts LG, Squire VA. 2012b. On the calculation of an attenuation coefficient for transects of ice-covered ocean. *Proc. R. Soc. A* 468:136–62

Bennetts LG, Williams TD. 2010. Wave scattering by ice floes and polynyas of arbitrary shape. *J. Fluid Mech.* 662:5–35

Bennetts LG, Williams TD. 2015. Water wave transmission by an array of floating discs. *Proc. R. Soc. A* 471:20140698

Boutin G, Ardhuin F, Dumont D, Svigny C, Girard-Ardhuin F, Accensi M. 2018. Floe size effect on wave-ice interactions: possible effects, implementation in wave model, and evaluation. *J. Geophys. Res. Oceans* 123:4779–805

Bukatov AE. 2017. *Volny v more s plavayushchim ledyanym pokrovom* [*Waves in the Sea with a Floating Ice Cover*]. Sevastopol, Rus.: Mar. Hydrophys. Inst. **http://mhi-ras.ru/news/news_201802151133.html**

Cheng S, Rogers WE, Thomson J, Smith M, Doble MJ, et al. 2017. Calibrating a viscoelastic sea ice model for wave propagation in the Arctic fall marginal ice zone. *J. Geophys. Res. Oceans* 122:8770–93

Collins C, Doble MJ, Lund B, Smith M. 2018. Observations of surface wave dispersion in the marginal ice zone. *J. Geophys. Res. Oceans* 123:3336–54

Collins CO, Rogers WE, Marchenko A, Babanin AV. 2015. In situ measurements of an energetic wave event in the Arctic marginal ice zone. *Geophys. Res. Lett.* 42:1863–70

De Santi F, De Carolis G, Olla P, Doble MJ, Cheng S, et al. 2018. On the ocean wave attenuation rate in grease-pancake ice, a comparison of viscous layer propagation models with field data. *J. Geophys. Res. Oceans* 123:5933–48

De Santi F, Olla P. 2017. Effect of small floating disks on the propagation of gravity waves. *Fluid Dyn. Res.* 49:025512

Deser C, Walsh JE, Timlin MS. 2000. Arctic sea ice variability in the context of recent atmospheric circulation trends. *J. Climate* 13:617–33

Doble MJ, De Carolis G, Meylan MH, Bidlot JR, Wadhams P. 2015. Relating wave attenuation to pancake ice thickness, using field measurements and model results. *Geophys. Res. Lett.* 42:4473–81

Dolatshah A, Nelli F, Bennetts LG, Alberello A, Meylan MH, et al. 2018. Letter: Hydroelastic interactions between water waves and floating freshwater ice. *Phys. Fluids* 30:091702

Dumont D, Kohout A, Bertino L. 2011. A wave-based model for the marginal ice zone including a floe breaking parameterization. *J. Geophys. Res. Oceans* 116:C04001

Fox C, Squire VA. 1994. On the oblique reflexion and transmission of ocean waves from shore fast sea ice. *Philos. Trans. R. Soc. A* 347:185–218

Hegarty GM, Squire VA. 2008. A boundary-integral method for the interaction of large-amplitude ocean waves with a compliant floating raft such as a sea-ice floe. *J. Eng. Math.* 62:355–72

Kagemoto H, Yue DKP. 1986. Interactions among multiple three-dimensional bodies in water waves: an exact algebraic method. *J. Fluid Mech.* 166:189–209

Keller JB. 1998. Gravity waves on ice-covered water. *J. Geophys. Res. Oceans* 103:7663–70

Kohout AL, Meylan MH. 2008. An elastic plate model for wave attenuation and ice floe breaking in the marginal ice zone. *J. Geophys. Res. Oceans* 113:C09016

Kohout AL, Meylan MH, Plew DR. 2011. Wave attenuation in a marginal ice zone due to the bottom roughness of ice floes. *Ann. Glaciol.* 52:118–22

Kohout AL, Meylan MH, Sakai S, Hanai K, Leman P, Brossard D. 2007. Linear water wave propagation through multiple floating elastic plates of variable properties. *J. Fluid Struct.* 23:649–63

Kohout AL, Williams MJM, Dean SM, Meylan MH. 2014. Storm-induced sea-ice breakup and the implications for ice extent. *Nature* 509:604–7

Li J, Kohout AL, Doble MJ, Wadhams P, Guan C, Shen HH. 2017. Rollover of apparent wave attenuation in ice covered seas. *J. Geophys. Res. Oceans* 122:8557–66
Li J, Kohout AL, Shen HH. 2015a. Comparison of wave propagation through ice covers in calm and storm conditions. *Geophys. Res. Lett.* 42:5935–41
Li J, Mondal S, Shen HH. 2015b. Sensitivity analysis of a viscoelastic parameterization for gravity wave dispersion in ice covered seas. *Cold Reg. Sci. Technol.* 120:63–75
Liu Q, Babanin AV, Zieger S, Young IR, Guan C. 2016. Wind and wave climate in the Arctic ocean as observed by altimeters. *J. Climate* 29:7957–75
Massom RA, Scambos TA, Bennetta LG, Reid P, Squire VA, Stammerjohn SE. 2018. Antarctic ice shelf disintegration triggered by sea ice loss and ocean swell. *Nature* 558:383–89
Meylan MH, Bennetts LG. 2018. Three-dimensional time-domain scattering of waves in the marginal ice zone. *Philos. Trans. R. Soc. A* 376(2129): 20170334
Meylan MH, Bennetts LG, Cavaliere C, Alberello A, Toffoli A. 2015a. Experimental and theoretical models of wave-induced flexure of a sea ice floe. *Phys. Fluids* 27:041704
Meylan MH, Bennetts LG, Kohout AL. 2014. In situ measurements and analysis of ocean waves in the Antarctic marginal ice zone. *Geophys. Res. Lett.* 41:5046–51
Meylan MH, Bennetts LG, Mosig JEM, Rogers WE, Doble MJ, Peter MA. 2018. Dispersion relations, power laws, and energy loss for waves in the marginal ice zone. *J. Geophys. Res. Oceans* 123:3322–35
Meylan MH, Yiew LJ, Bennetts LG, French BJ, Thomas GA. 2015b. Surge motion of an ice floe in waves: comparison of a theoretical and an experimental model. *Ann. Glaciol.* 56:155–59
Montiel F, Bennetts LG, Squire VA, Bonnefoy F, Ferrant P. 2013a. Hydroelastic response of floating elastic discs to regular waves. Part 2. Modal analysis. *J. Fluid Mech.* 723:629–52
Montiel F, Bonnefoy F, Ferrant P, Bennetts LG, Squire VA, Marsault P. 2013b. Hydroelastic response of floating elastic discs to regular waves. Part 1. Wave basin experiments. *J. Fluid Mech.* 723:604–28
Montiel F, Squire VA. 2017. Modelling wave-induced sea ice break-up in the marginal ice zone. *Proc. R. Soc. A* 473:20170258
Montiel F, Squire VA, Bennetts LG. 2015a. Evolution of directional wave spectra through finite regular and randomly perturbed arrays of scatterers. *SIAM J. Appl. Math.* 75:630–51
Montiel F, Squire VA, Bennetts LG. 2015b. Reflection and transmission of ocean wave spectra by a band of randomly distributed ice floes. *Ann. Glaciol.* 56:315–22
Montiel F, Squire VA, Bennetts LG. 2016. Attenuation and directional spreading of ocean wave spectra in the marginal ice zone. *J. Fluid Mech.* 790:492–522
Montiel F, Squire VA, Doble MJ, Thomson J, Wadhams P. 2018. Attenuation and directional spreading of ocean waves during a storm event in the autumn Beaufort Sea marginal ice zone. *J. Geophys. Res. Oceans* 123:5912–32
Mosig JEM, Montiel F, Squire VA. 2015. Comparison of viscoelastic-type models for ocean wave attenuation in ice-covered seas. *J. Geophys. Res. Oceans* 120:6072–90
Nelli F, Bennetts LG, Skene DM, Monty JP, Lee JH, et al. 2017. Reflection and transmission of regular water waves by a thin, floating plate. *Wave Motion* 70:209–21
NSIDC (Natl. Snow Ice Data Center). 2006. *Submarine upward looking sonar ice draft profile data and statistics, version 1*. Data Set, Natl. Snow Ice Data Center, Boulder, CO. **http://nsidc.org/data/g01360.html**
Peter MA, Meylan MH. 2007. Water-wave scattering by a semi-infinite periodic array of arbitrary bodies. *J. Fluid Mech.* 575:473–94
Rabault J, Sutherland G, Gundersen O, Jensen A. 2017. Measurements of wave damping by a grease ice slick in Svalbard using off-the-shelf sensors and open-source electronics. *J. Glaciol.* 63:372–81
Roach LA, Smith MM, Dean SM. 2018. Quantifying growth of pancake sea ice floes using images from drifting buoys. *J. Geophys. Res. Oceans* 123:2851–66
Rogers WE, Thomson J, Shen HH, Doble MJ, Wadhams P, Cheng S. 2016. Dissipation of wind waves by pancake and frazil ice in the autumn Beaufort Sea. *J. Geophys. Res. Oceans* 121:7991–8007
Shen H, Perrie W, Hu Y, He Y. 2018. Remote sensing of waves propagating in the marginal ice zone by SAR. *J. Geophys. Res. Oceans* 123:189–200

Shen HH. 2017. Wave–ice interactions. In *Encyclopedia of Maritime and Offshore Engineering*, ed. J Carlton, P Jukes, YS Choo. Hoboken, NJ: Wiley. **https://doi.org/10.1002/9781118476406.emoe086**
Skene D, Bennetts L, Meylan M, Toffoli A. 2015. Modelling water wave overwash of a thin floating plate. *J. Fluid Mech.* 777:R3
Squire VA. 2007. Of ocean waves and sea-ice revisited. *Cold Reg. Sci. Technol.* 49:110–133
Squire VA. 2018. A fresh look at how ocean waves and sea ice interact. *Philos. Trans. R. Soc. A* 376:20170342
Squire VA, Allan AJ. 1980. Propagation of flexural gravity waves in sea ice. In *Sea Ice Processes and Models*, ed. RS Pritchard, pp. 327–38. Seattle: Univ. Wash. Press
Squire VA, Dugan JP, Wadhams P, Rottier PJ, Liu AK. 1995. Of ocean waves and sea ice. *Annu. Rev. Fluid Mech.* 27:115–68
Squire VA, Montiel F. 2016. Evolution of directional wave spectra in the marginal ice zone: a new model tested with legacy data. *J. Phys. Oceanogr.* 46:3121–37
Squire VA, Moore SC. 1980. Direct measurement of the attenuation of ocean waves by pack ice. *Nature* 283:365–68
Squire VA, Vaughan GL, Bennetts LG. 2009. Ocean surface wave evolvement in the Arctic Basin. *Geophys. Res. Lett.* 36:L22502
Squire VA, Williams TD. 2008. Wave propagation across sea-ice thickness changes. *Ocean Model.* 21(1-2): 1–11
Stopa JE, Ardhuin F, Thomson J, Smith MM, Kohout AL, et al. 2018a. Wave attenuation through an Arctic marginal ice zone on 12 October 2015: 1. Measurement of wave spectra and ice features from Sentinel 1A. *J. Geophys. Res. Oceans* 123:3619–34
Stopa JE, Sutherland P, Ardhuin F. 2018b. Strong and highly variable push of ocean waves on Southern Ocean sea ice. *PNAS* 115:5861–65
Stroeve J, Holland MM, Meier W, Scambos T, Serreze M. 2007. Arctic sea ice decline: faster than forecast. *Geophys. Res. Lett.* 34:L09501
Sutherland BR, Balmforth NJ. 2019. Damping of surface waves by floating particles. *Phys. Rev. Fluids* 4:014804
Sutherland G, Rabault J. 2016. Observations of wave dispersion and attenuation in landfast ice. *J. Geophys. Res. Oceans* 121:1984–97
Sutherland G, Rabault J, Christensen KH, Jensen A. 2018. A two layer model for wave dissipation in sea ice. arXiv:1805.01134 [physics.ao-ph]
Sutherland P, Brozena JE, Doble MJ, Wadhams P. 2018. Airborne remote sensing of wave propagation in the marginal ice zone. *J. Geophys. Res. Oceans* 123:4132–52
Thomson J, Ackley S, Girard-Ardhuin F, Ardhuin F, Babanin A, et al. 2018. Overview of the Arctic Sea State and Boundary Layer Physics program. *J. Geophys. Res. Oceans* 123:8674–87
Thomson J, Squire VA, Ackley S, Rogers E, Babanin A, et al. 2013. *Science plan: Sea State and Boundary Layer Physics of the Emerging Arctic Ocean*. Tech. Rep. 1306, Appl. Phys. Lab., Univ. Wash., Seattle, WA
Toffoli A, Bennetts LG, Meylan MH, Cavaliere C, Alberello A, et al. 2015. Sea ice floes dissipate the energy of steep ocean waves. *Geophys. Res. Lett.* 42:8547–54
Vaughan GL, Bennetts LG, Squire VA. 2009. The decay of flexural-gravity waves in long sea ice transects. *Proc. R. Soc. A* 465:2785–812
Vaughan GL, Squire VA. 2007. Scattering of ice-coupled waves by a sea-ice sheet with random thickness. *Wave Random Complex* 17:357–80
Vaughan GL, Squire VA. 2008. Ocean wave scattering by natural sea ice transects. *J. Geophys. Res. Oceans* 113:C10022
Wadhams P, Aulicino G, Parmiggiani F, Persson POG, Holt B. 2018. Pancake ice thickness mapping in the Beaufort Sea from wave dispersion observed in SAR imagery. *J. Geophys. Res. Oceans* 123:2213–37
Wadhams P, Doble MJ. 2009. Sea ice thickness measurement using episodic infragravity waves from distant storms. *Cold Reg. Sci. Technol.* 56:98–101
Wadhams P, Holt B. 1991. Waves in frazil and pancake ice and their detection in Seasat synthetic aperture radar imagery. *J. Geophys. Res. Oceans* 96:8835–52
Wadhams P, Lange M, Ackley SF. 1987. The ice thickness distribution across the Atlantic sector of the Antarctic Ocean in midwinter. *J. Geophys. Res. Oceans* 92:14535–52

Wadhams P, Squire VA, Ewing JA, Pascal RW. 1986. The effect of the marginal ice zone on the directional wave spectrum of the ocean. *J. Phys. Oceanogr.* 16:358–76

Wadhams P, Squire VA, Goodman DJ, Cowan AM, Moore SC. 1987. The attenuation of ocean waves in the marginal ice zone. *J. Geophys. Res. Oceans* 93:6799–818

Wang CD, Meylan MH, Porter R. 2007. The linear-wave response of a periodic array of floating elastic plates. *J. Eng. Math.* 57:23–40

Wang R, Shen HH. 2010. Gravity waves propagating into an ice-covered ocean: a viscoelastic model. *J. Geophys. Res. Oceans* 115:C06024

Wang R, Shen HH. 2011. A continuum model for the linear wave propagation in ice-covered oceans: an approximate solution. *Ocean Model.* 38:244–50

Weeks WF. 2010. *On Sea Ice*. Fairbanks, AK: Univ. Alsk. Press

Williams TD, Bennetts LG, Squire VA, Dumont D, Bertino L. 2013a. Wave–ice interactions in the marginal ice zone. Part 1: theoretical foundations. *Ocean Model.* 71:81–91

Williams TD, Bennetts LG, Squire VA, Dumont D, Bertino L. 2013b. Wave–ice interactions in the marginal ice zone. Part 2: numerical implementation and sensitivity studies along 1D transects of the ocean surface. *Ocean Model.* 71:92–101

Williams TD, Rampal P, Bouillon S. 2017. Wave–ice interactions in the neXtSIM sea-ice model. *Cryosphere* 11:2117–35

Williams TD, Squire VA. 2008. The effect of submergence on wave scattering across a transition between two floating flexible plates. *Wave Motion* 45:361–79

Williams TD, Squire VA. 2010. On the estimation of ice thickness from scattering observations. *Dynam. Atmos. Oceans* 49:215–33

WW3DG (WAVEWATCH III® Dev. Group). 2016. *User manual and system documentation of WAVEWATCH III® version 5.16*. Tech. Note 329, NOAA (Natl. Ocean. Atmos. Admin.)/NWS (Natl. Weather Serv.)/NCEP (Natl. Center Environ. Protect.)/MMAB (Mar. Model. Anal. Branch), College Park, MD

Yiew LJ, Bennetts LG, Meylan MH, French BJ, Thomas GA. 2016. Hydrodynamic responses of a thin floating disk to regular waves. *Ocean Model.* 97:52–64

Yiew LJ, Bennetts LG, Meylan MH, Thomas GA, French BJ. 2017. Wave-induced collisions of thin floating disks. *Phys. Fluids* 29:127102

Young IR, Zieger S, Babanin AV. 2011. Global trends in wind speed and wave height. 332:451–55

Zhao X, Cheng S, Shen HH. 2017. Nature of wave modes in a coupled viscoelastic layer over water. *J. Eng. Mech.* 143:04017114

Zhao X, Shen HH. 2013. Ocean wave transmission and reflection between two connecting viscoelastic ice covers: an approximate solution. *Ocean Model.* 71:102–13

Zhao X, Shen HH. 2015a. Ocean wave transmission and reflection by viscoelastic ice covers. *Ocean Model.* 92:1–10

Zhao X, Shen HH. 2015b. Wave propagation in frazil/pancake, pancake, and fragmented ice covers. *Cold Reg. Sci. Technol.* 113:71–80

Zhao X, Shen HH. 2018. Three-layer viscoelastic model with eddy viscosity effect for flexural-gravity wave propagation through ice cover. *Ocean Model.* 131:15–23

Zhao X, Shen HH, Cheng S. 2015. Modeling ocean wave propagation under sea ice covers. *Acta Mech. Sin.* 31:1–15